Pergamon

Geochimica et Cosmochimica Acta, Vol. 66, No. 12, pp. 2267–2272, 2002

0016-7037/02 $22.00 + .00

PII S0016-7037(01)00835-3

A possible effect of melt structure on the Mg-Fe^{2+} partitioning between olivine and melt

IKUO KUSHIRO[†,*] and BJORN O. MYSEN

Geophysical Laboratory, Carnegie Institution of Washington, Washington, D.C. 20015-1305, USA

(*Received May* 3, 2001; *accepted in revised form October* 4, 2001)

Abstract—Partitioning of Mg and Fe^{2+} between olivine and mafic melts has been determined experimentally for eight different synthetic compositions in the temperature range between 1335 and 1425°C at 0.1 MPa pressure and at fo_2 ~1 log unit below the quartz-fayalite-magnetite buffer. The partition coefficient [$K_D = (Fe^{2+}/Mg)^{ol}/(Fe^{2+}/Mg)^{melt}$] increases from 0.25 to 0.34 with increasing depolymerization of melt (NBO/T of melt from 0.25–1.2), and then decreases with further depolymerization of melt (NBO/T from 1.2–2.8). These variations are similar to those observed in natural basalt-peridotite systems. In particular, the variation in NBO/T ranges for basaltic-picritic melts (0.4–1.5) is nearly identical to that obtained in the present experiments. Because the present experiments were carried out at constant pressure (0.1 MPa) and in a relatively small temperature range (90°C), the observed variations of Mg and Fe^{2+} partitioning between olivine and melt must depend primarily on the composition or structure of melt. Such variations of K_D may depend on the relative proportions of four-, five-, and six-coordinated Mg^{2+} and Fe^{2+} in melt as a function of degree of NBO/T. *Copyright © 2002 Elsevier Science Ltd*

1. INTRODUCTION

Partitioning of Mg and Fe^{2+} between olivine and basaltic melts has been used widely in igneous petrology, particularly to identify primary magmas formed in the mantle and to estimate the composition of mantle peridotites (e.g., Roeder and Emslie, 1970). Based on theoretical and experimental studies, the partition coefficient, K_D [$(Fe^{2+}/Mg)^{ol}/(Fe^{2+}/Mg)^{melt}$], is known to change with temperature, pressure, and composition of melt. A number of investigators have suggested that the composition of melt is the major factor controlling the Mg-Fe^{2+} partitioning between olivine and melt (e.g., Longhi et al., 1978; Takahashi, 1978; Ford et al., 1983; Jones, 1984; Gee and Sack, 1988; Kushiro and Walter, 1998). Recently, Kushiro and Walter (1998) showed, based on the melting experiments of peridotite, that K_D increases with increasing MgO+FeO or degree of depolymerization of melt, reaches a maximum, and then decreases with a further increase of MgO+FeO or depolymerization of melt (NBO/T). Kushiro and Walter (1998) suggested that the degree of polymerization of melt would be a major factor in the partitioning of Mg and Fe^{2+} between olivine and melt. In most of these experiments, however, the composition of melt, temperature, and pressure varies simultaneously. The individual effect of temperature, pressure, and melt composition, therefore, could not be isolated. In the present experiments, pressure is fixed at 0.1 MPa, and the temperature range is restricted to a relatively narrow interval. The composition of melt is varied widely by using several different synthetic systems so that the effect of composition of melt on Mg-Fe^{2+} partitioning between olivine and melt can be evaluated.

2. EXPERIMENTS

Starting materials were eight different synthetic mixtures in the systems olivine-diopside-silica, olivine-anorthite-silica, olivine-diopside-akermanite, olivine-nepheline-silica, and olivine-leucite-silica. The proportions of endmember components in the mixtures are given in Table 1. The compositions of the mixtures were selected to cover a wide range in the degree of polymerization or NBO/T (non-bridging oxygen/tetrahedrally coordinated cations) and to have olivine on the liquidus at temperatures between 1300 and 1450°C. The NBO/T of the mixtures ranged from 0.51 to 3.05, which corresponds to those of basaltic to ultramafic compositions (Mysen, 1990). In these compositions the forsterite/fayalite ratio (Fo/Fa) ranged from 4.0 to 4.5 except for FNQ (Fo/Fa = 5.90). The Mg# [Mg# = 100Mg/(Mg+Fe)] of the mixtures ranged from 85.5 to 91.4.

Experiments were made at 0.1 MPa in vertical $MoSi_2$ quench furnaces. The wire-loop method was applied to all runs. The hanging wire was a Pt-Fe alloy, which was made by heating Pt wire (0.1 mm in diameter) with fine Fe metal powder for 24 h at 1150°C and at fo_2 below the quartz-fayalite-magnetite buffer, followed by dissolution in hydrochloric acid of unreacted iron surrounding the wire. The experiments were conducted at temperatures between 1335 and 1425°C and at fo_2 ~1 log unit lower than the quartz-fayalite-magnetite buffer to ensure that most of the Fe was in the divalent state. ^{57}Fe Mössbauer spectrum was taken for a glass formed from composition FAQ1 at 1400°C at −7.5 log fo_2 (Fig. 1). As shown in the figure, no measurable amount of ferric iron was detected in this glass. The fo_2 during the experiments was measured and monitored by an yttria-stabilized ZrO_2 cell (Sato, 1972). The run duration ranged from 15 to 26 h except for time-study experiments, which were made for 46 and 73 h (Table 2). The charges were quenched in water by electrically breaking the hanging wire. After quenching, the charges in most of the runs consisted of glass and olivine 10- to 30-μm across.

Analyses of olivine and glass were made with JEOL 8800 and 833 electron microprobes (Geophysical Laboratory and the University of Tokyo) operating in wavelength-dispersive mode. The accelerating voltage was 15 kV, and beam currents were 5 and 3 nA for analyses of olivine and alkali-free glasses and 1.2 nA for analyses of alkali-containing glasses.

3. RESULTS AND DISCUSSION

The results of the analyses are shown in Table 3. Both olivine and glass are homogeneous in each experiment with standard deviations < 1% for all of the analyses of both phases

* Author to whom correspondence should be addressed (ikushiro@ruby.ocn.ne.jp).
† *Present address:* Institute for Frontier Research on Earth Evolution (IFREE), Japan Marine Science and Technology Center, Yokosuka 237-0061, Japan

Table 1. Compositions of starting materials (proportion of each component in wt.%).

	FLQ1	FLQ2	FNQ	FAQ1	FAQ2	FDAQ	FD	FDAk
Forsterite (Mg_2SiO_4)	19.1	36.7	56.6	34.3	49.3	47.1	45.0	25.8
Fayalite (Fe_2SiO_4)	4.6	8.3	9.6	8.4	10.8	10.5	10.0	6.1
Diopside ($CaMgSi_2O_6$)						22.4	45.0	23.5
Akermanite ($Ca_2MgSi_2O_7$)								44.6
Anorthite ($CaAl_2Si_2O_8$)				50.4	27.9	14.0		
Nepheline ($NaAlSiO_4$)			22.2					
Leucite ($KAlSi_2O_6$)	59.8	27.5						
Quartz (SiO_2)	16.5	27.5	11.6	6.9	12.0	6.0		
NBO/T	0.51	1.11	1.91	1.04	2.00	2.45	2.99	3.04

except for glass in run number 10 (1.9%). Based on these values, the uncertainty of K_D is estimated to be $< 2\%$. The FeO contents of glass, however, changed in some of the experiments probably due to diffusion of iron from or into iron-soaked Pt wire. For example, the charge of run number 34, consisting only of glass, has 3.83 wt.% FeO, as compared to 3.36% wt.% in the starting material.

Time-study experiments were carried out for starting materials FAQ1 and FD. For composition FAQ1, the FeO contents of glass were 9.51 and 10.38% for 24 and 73 h, respectively (nos. 7 and 33), whereas for composition FD, the FeO contents were 8.45, 8.38, and 8.19% for 4, 24, and 46.5 h, respectively (nos. 30, 25, 32; Table 3). Despite such FeO variations in glass, the calculated K_D was relatively constant for respective compositions at fixed temperature: 0.327 and 0.329 for composition FAQ1 and 0.290, 0.300, and 0.305 for composition FD.

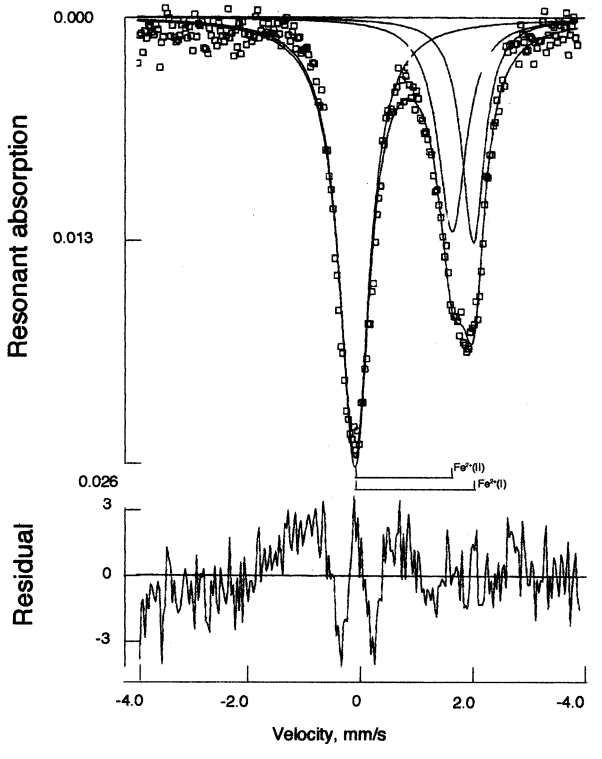

Fig. 1. ^{57}Fe resonant absorption Mössbauer spectrum of a glass quenched from melt of FAQ1 composition at -7.5 log fo_2 and at 1400°C, showing no detactable amount of Fe^{3+}.

Concerning the oxidation state of iron, although no measurable amount of Fe^{3+} was detected in the ^{57}Fe Mössbauer spectrum of one of the quenched melts (Fig. 1), there is a possibility that small amounts of Fe^{3+} may exist in this and other melts under the present experimental conditions. The $Fe^{3+}/(Fe^{3+} + Fe^{2+})$ in the melts was estimated with the formulation of Kilinc et al. (1983). Despite the fact that this formulation is based on the calibration of ferric/ferrous from natural rock compositions and does not take into account composition parameters such as SiO_2 and MgO, the results (Table 3) show that the melts have Fe^{3+}/Fe^{2+} ratios < 0.03 except for two melts with high CaO contents (0.036 and 0.033). This is consistent with the ^{57}Fe Mössbauer spectrum.

The K_D obtained on the assumption that Fe in melts is all Fe^{2+} ranges from 0.248 to 0.352 (Table 3). Because all the experiments were performed at 0.1 MPa and in a relatively narrow temperature range (1335–1425°C), such a large variation in K_D would most probably be due to the compositional variation of melt. K_D was also obtained by using the calculated

Table 2. Conditions of experiments.

Run no.	Starting material	Temperature (°C)	Log fo2	Time (hr)	Phases
34	FLQ1	1400	−7.5	26	G1
12	FLQ1	1375	−7.8	24	G1+O1
5	FLQ1	1360	−7.8	24	G1+O1
31	FLQ2	1425	−6.9	21	G1+O1
13	FLQ2	1400	−7.5	24	G1+O1
10	FLQ2	1375	−7.8	15.5	G1+O1
29	FNQ	1425	−6.9	19.2	G1+O1
19	FNQ	1410	−7.5	24	G1+O1
20	FNQ	1350	−7.8	26.3	G1+O1
21	FNQ	1335	−8.2	24.8	G1+O1
1	FAQ1	1410	−7.5	23.8	G1
11	FAQ1	1360	−7.8	25.8	G1
22	FAQ1	1335	−8.2	24	G1+O1
28	FAQ2	1415	−6.9	23.5	G1+O1
24	FAQ2	1390	−7.8	24	G1+O1
7	FAQ2	1360	−7.8	24	G1+O1
33	FAQ2	1360	−7.8	73	G1+O1
15	FAQ2	1335	−8.2	26	G1+O1
9	FD	1410	−7.5	18.5	G1+O1
30	FD	1375	−7.8	4	G1+O1
25	FD	1375	−7.8	24	G1+O1
32	FD	1375	−7.8	46.5	G1+O1
27	FDAk	1425	−6.9	21.2	G1+O1
14	FDAk	1400	−7.5	24.3	G1+O1
8	FDAk	1375	−7.8	24	G1+O1
23	FDAk	1350	−7.8	24	G1+O1
35	FDAQ	1375	−7.8	22	G1+O1

Table 3. Compositions of olivine and glass.

Run no.	Starting material	Olivine	Glass											
		Mg#	SiO_2	Al_2O_3	FeO	MgO	CaO	Na_2O	K_2O	Mg#	NBO/T	K_D	Fe^{3+}/Fe^{2+}*	K_D**
12	FLQ1	91.56 (10)	61.69	16.31	4.22	6.50			11.29	73.30 (10)	0.27	0.253 (1)	0.0204	0.263
5	FLQ1	92.16 (6)	61.55	15.72	4.63	7.84			10.26	75.12 (68)	0.32	0.257 (2)	0.0206	0.267
31	FLQ2	93.35 (18)	65.08	7.55	6.50	16.03			4.85	81.49 (32)	0.76	0.314 (2)	0.0189	0.325
13	FLQ2	89.71 (2)	70.08	9.47	5.48	7.84			7.13	71.84 (38)	0.38	0.293 (2)	0.0177	0.303
10	FLQ2	89.31 (64)	73.64	9.66	4.01	5.07			7.62	69.26 (129)	0.24	0.270 (7)	0.0173	0.279
29	FNQ	93.89 (14)	54.02	10.64	9.11	25.47		0.75		83.30 (41)	1.22	0.325 (2)	0.0149	0.334
19	FNQ	92.74 (5)	54.91	12.04	9.15	23.07		0.83		81.82 (16)	1.05	0.352 (1)	0.0117	0.360
20	FNQ	91.22 (2)	59.92	15.98	7.15	13.33		3.62		76.86 (3)	0.51	0.320 (1)	0.0155	0.330
21	FNQ	91.34 (3)	61.62	15.60	6.76	12.53		3.49		76.74 (23)	0.47	0.313 (1)	0.0135	0.322
22	FAQ1	93.90 (13)	46.12	19.77	6.51	16.66	10.95			82.02 (10)	0.88	0.296 (1)	0.0137	0.304
28	FAQ2	93.30 (6)	50.34	12.22	8.61	22.09	6.74			82.05 (19)	1.25	0.328 (1)	0.0176	0.340
24	FAQ2	92.85 (5)	50.51	12.59	8.78	21.09	7.04			81.08 (13)	1.20	0.330 (1)	0.0126	0.338
7	FAQ2	92.13 (5)	50.31	12.68	9.51	20.45	7.05			79.30 (22)	1.19	0.327 (1)	0.0146	0.337
33	FAQ2	91.04 (6)	49.72	13.03	10.38	19.50	7.38			77.00 (56)	1.18	0.329 (3)	0.0149	0.339
15	FAQ2	91.12 (3)	52.00	14.58	8.80	16.51	8.12			76.98 (62)	0.94	0.326 (3)	0.0136	0.335
9	FD	92.93 (6)	49.85		9.99	22.29	17.87			79.89 (17)	2.47	0.302 (1)	0.0213	0.315
30	FD	93.44 (8)	51.68		8.45	19.58	20.30			80.52 (66)	2.27	0.290 (3)	0.0227	0.303
25	FD	93.02 (4)	52.01		8.38	18.81	20.80			80.00 (35)	2.23	0.300 (1)	0.0231	0.314
32	FD	93.34 (7)	51.87		8.19	19.65	20.29			81.04 (47)	2.26	0.305 (2)	0.0227	0.319
27	FDAk	96.67 (1)	46.37		4.75	19.18	29.70			87.79 (48)	2.81	0.248 (1)	0.0356	0.266
14	FDAk	96.31 (8)	46.45		5.03	18.45	30.08			86.75 (36)	2.79	0.251 (1)	0.0299	0.265
8	FDAk	95.48 (9)	46.82		5.73	17.51	29.95			84.48 (27)	2.72	0.258 (1)	0.0292	0.273
23	FDAk	95.44 (16)	47.79		5.28	17.06	29.87			85.23 (27)	2.62	0.276 (1)	0.0328	0.293
35	FDAQ	93.55 (7)	51.59	7.66	7.71	19.96	13.08			82.20 (20)	1.52	0.318 (1)	0.0169	0.329

Numbers in parentheses indicate standard error of the mean uncertainty.
* Calculated using an empirical formulation of Kilinc et al. (1983).
** Calculated using Fe^{2+}/Fe^{3+} given above.

Fe^{3+}/Fe^{2+} ratios in the melts (Table 3). The latter K_D ranges from 0.266 to 0.360 and is 2 to 5% larger than the former K_D. Figure 2 shows the variation of K_D as a function of NBO/T of glass (NBO/T is calculated from glass composition as described by Mysen et al., 1982). The K_D increases from 0.25 to 0.26 at NBO/T ~0.2 to ~0.33 to 0.34 at NBO/T ~1.0 to 1.2 (the highest is ~0.36), and then decreases to 0.25 to 0.27 when the NBO/T further increases to 2.8. Although K_D scatters at NBO/T between 0.8 and 1.2, a smooth convex curve with a maximum at ~1.2 NBO/T can be well fitted to most of the points, having a correlation coefficient, R, of 0.900. Correlation of K_D with other compositional parameters is also examined. Major oxides contained in all the starting materials are SiO_2, MgO, and FeO. Plots of K_D against SiO_2 and MgO+FeO are quite scattered and the correlation factors are significantly smaller than that for NBO/T ($R = 0.356$ and 0.646, respectively). These results suggest that NBO/T or degree of polymerization of melt would be most closely related to the partitioning of Mg and Fe^{2+} between olivine and melt.

Alkalis may cause a decrease of K_D as discussed by several investigators (e.g., Gee and Sack, 1988; Carmichael and Ghiorso, 1990; Falloon et al., 1997; Sugawara, 1998). The data compiled by Falloon et al. (1997) and Sugawara (1998) indicate that this effect is evident when Na_2O+K_2O is $>$ 6 to 7 wt.%. In the present study, low K_D values (< 0.28) were obtained for both low and high NBO/T glasses. The former glasses with low NBO/T contained $>$ 7.5 wt.% K_2O (nos. 5, 10, and 12; Table 3), and lower K_D for these runs could be due to such high K_2O contents. It should be mentioned, however, that alkalis in the presence of alumina polymerize silicate melts (except for excess alkalis over alumina), because alkalis serve to charge-balance Al^{3+} in tetrahedral coordination. The lower K_D in these experiments, therefore, may result from a higher degree of polymerization (smaller NBO/T). The ultramafic glasses with high NBO/T (nos. 8, 14, 23, and 27; Table 3) contain large amounts of CaO ($>$ 29 wt.%), and one might suggest that such high CaO contents could be the cause of low K_D. Low K_D was also obtained, however, for ultramafic melts with 1.5 to 2.9 wt.% CaO in the melting of peridotite (Kushiro and Walter, 1998), and CaO should not be the direct cause of low K_D. These high CaO melts have no alumina, and one might also suggest that a contrastive negative trend shown by these melts could be due to the absence of alumina. However, a negative trend is also observed for natural peridotitic melts containing significant amounts of alumina (Kushiro and Walter, 1998) and should not be due to the absence of alumina.

In the natural basalt-peridotite system, which also covers a broad range in temperature and pressure, K_D also increases with increasing NBO/T of melts, reaches a maximum, and decreases with a further increase of NBO/T (Kushiro and Walter, 1998). The shapes of the K_D-fitted curves for the basalt-peridotite and synthetic systems resemble one another. Figure 2 shows for comparison a second-order polynominal curve fitted to the data obtained in the basalt-peridotite system (Kushiro and Walter, 1998). It has a maximum in K_D at NBO/T of the melt of ~2, whereas the present synthetic melts show a maximum at NBO/T of between 1 and 1.5 (Fig. 2). The most relevant range of NBO/T for mafic magmas, such as basaltic

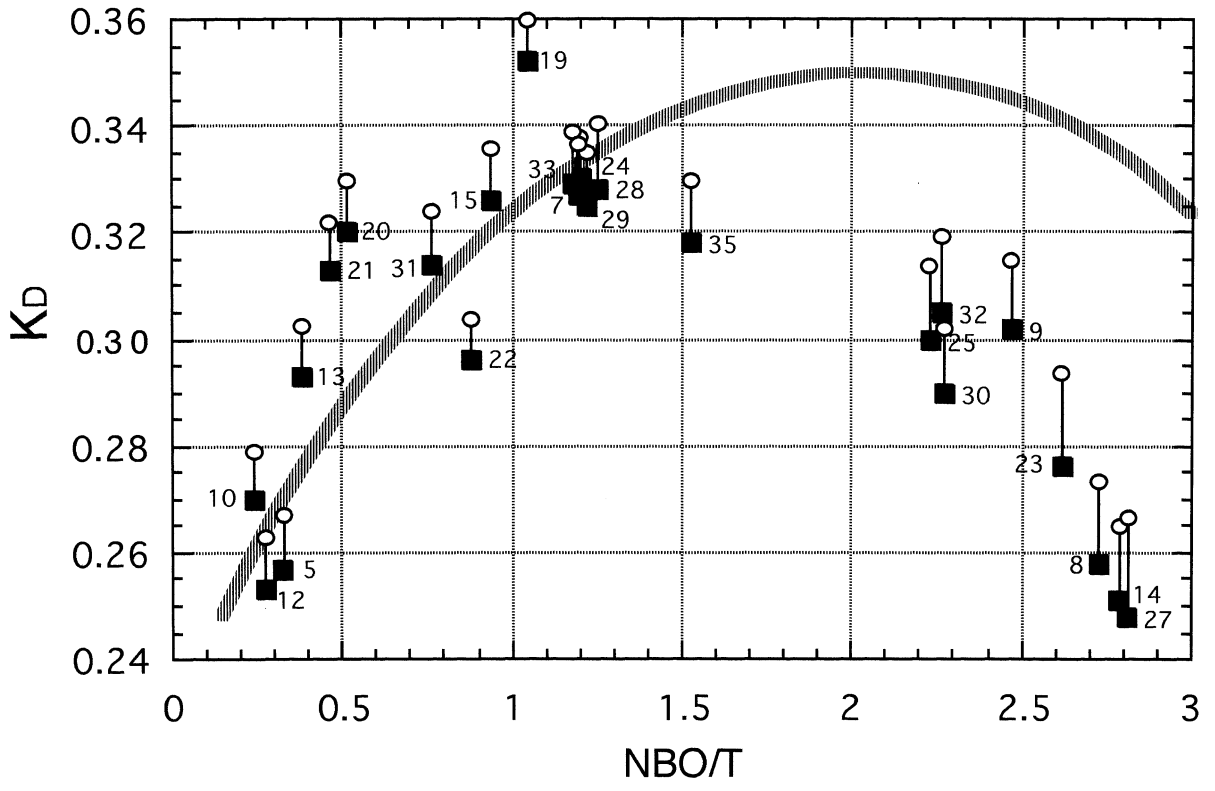

Fig. 2. Mg-Fe^{2+} partition coefficient K_D [$(Fe^{2+}/Mg)^{ol}/(Fe^{2+}/Mg)^{melt}$] for olivine-melt plotted against NBO/T (number of nonbridging oxygen/tetrahedrally coordinated cation). Solid squares indicate K_D obtained on the assumption that Fe in melts is all Fe^{2+}, and small open circles indicate K_D calculated by using Fe^{3+}/Fe^{2+} ratios in melts given in Table 3. Numbers denote the run numbers given in Table 2. Hatched curve is a second-order polynominal curve fitted to the K_D data obtained for partial melts from mantle peridotites (Kushiro and Walter; 1998).

and picritic magmas, is between 0.4 and 1.4, in which the variations of K_D obtained in the basalt-peridotite systems and the present synthetic systems are nearly identical. It is suggested that the variations of K_D observed in the basalt-peridotite systems are mainly due to the variation in the composition or structure of melts and that NBO/T would also be applicable to the K_D variations in natural mafic-ultramafic melts.

The difference between partial melts from peridotite and present synthetic melts at NBO/T $>$ 1.4 may be due to differences in temperature or pressure or both. The partial melts from peridotite with NBO/T $>$ 1.4 were obtained mostly at pressures $>$ 4 GPa and at temperatures $>$ 1600°C. Such high pressures and temperatures may result in larger K_D values than those of the present synthetic melts obtained at 0.1 MPa and at temperatures $<$ 1425°C.

Distribution coefficients for Mg and Fe between olivine and glass are shown as a function of NBO/T of glass (Fig. 3). The distribution coefficient for Mg ($D_{Mg} = Mg^{ol}/Mg^{melt}$) decreases from 9.6 to ~2 with increasing NBO/T from 0.2 to 1.2, and then increases slightly with a further increase of NBO/T. That of Fe ($D_{Fe} = Fe^{ol}/Fe^{2+melt}$) decreases from 2.61 to 0.68 (2.70–0.69 when Fe^{3+}/Fe^{2+} ratios in Table 3 are taken into account). The variations would also be due to the change in composition of melt, particularly the change in its degree of polymerization. These variations in D_{Mg} and D_{Fe} cover most of those for natural basalt-peridotite systems (Kushiro and Walter, 1998; Kushiro, 2001), which range from 8 to 1.8 for D_{Mg} and from 2 to 0.05 for D_{Fe} in the range of NBO/T from 0.4 to 3.0.

The parabolic relationship between K_D and NBO/T of the melt (Fig. 2) may be related to ordering of Fe^{2+} and Mg^{2+} among coexisting structural units in the melt. These structural units are characterized by the NBO/T of the individual units numbering one for Q^3, two for Q^2, three for Q^1, and four for Q^0. There also exists a fifth type of unit, Q^4, that has no nonbridging oxygen (Virgo et al., 1980; Schramm et al., 1984; Maekawa et al., 1991). The proportion of these units is a systematic function of melt composition (NBO/T), with Q^3 units showing maximum abundance in melts with NBO/T ~1 (see, e.g., Fig. 4 in Maekawa et al., 1991). For melts of fixed overall NBO/T, the abundance in particular of Q^3 units is correlated with the ionization potential of network-modifying cations in the melts (Mysen et al., 1982). We suggest that preferences of Fe^{2+} and Mg^{2+} among the various types of nonbridging oxygen in the melts are reflected in the relationship between K_D and the overall degree of melt polymerization (NBO/T), although how the preferences of Fe^{2+} and Mg^{2+} are related to particular types of structural units in melts is not known at present.

The difference in the rate of change of D with NBO/T (Fig. 3) and the change of K_D with NBO/T (Fig. 2) may be viewed from the structural sites of Mg^{2+} and Fe^{2+} in silicate melts. The studies with XAFS and EXAFS on silicate melts and

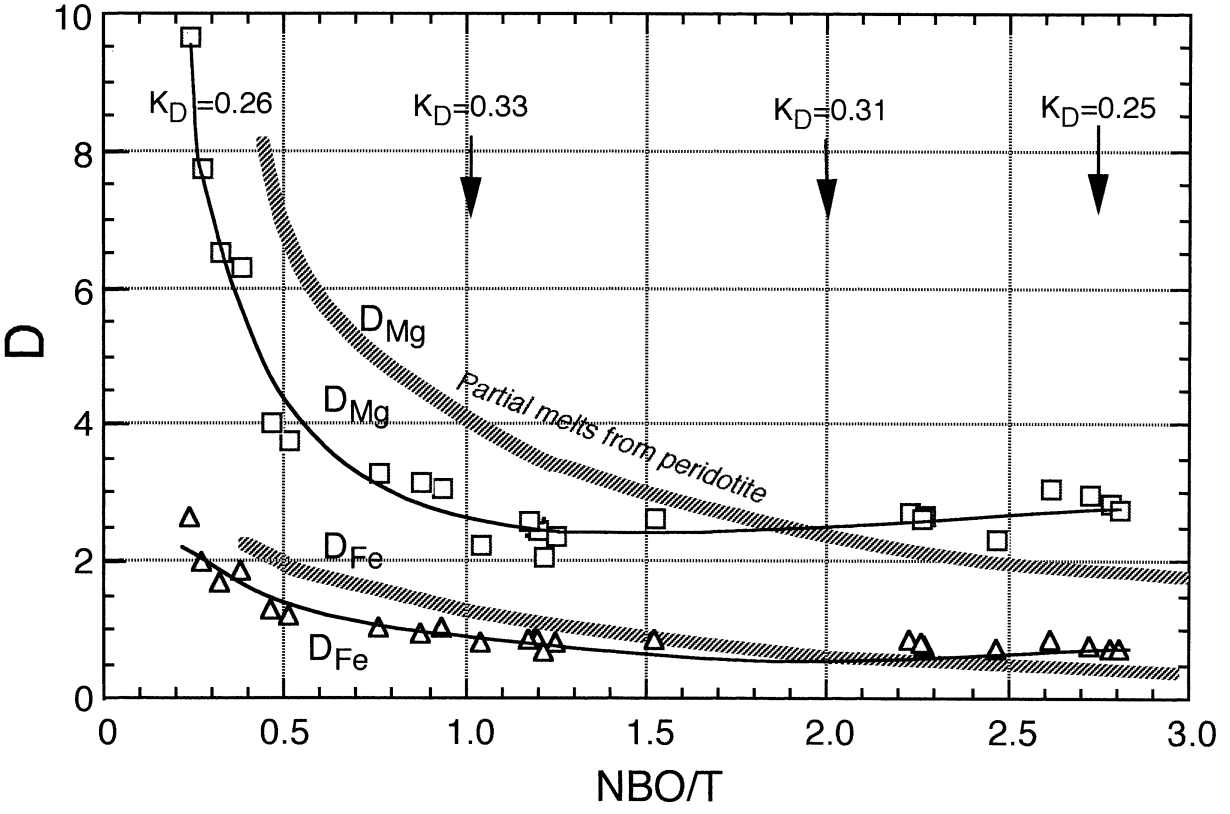

Fig. 3. Distribution coefficient D ($D_{Mg} = Mg^{ol}/Mg^{melt}$, $D_{Fe} = Fe^{ol}/Fe^{2+melt}$) for olivine-melt plotted against NBO/T. D_{Fe} here is calculated assuming all Fe as Fe^{2+}; however, the differences between this D_{Fe} and the D_{Fe} calculated using Fe^{3+}/Fe^{2+} ratios in Table 3 are so small that they are included within the size of the symbols. D_{Mg} and D_{Fe} for partial melts from peridotite (Kushiro, 2001) are shown for comparison.

glasses with several different mafic compositions indicate that Fe^{2+} and Mg^{2+} can be four-, five-, and six-coordinated with oxygen (for review, see Brown et al., 1995). The 25-magnesium NMR studies indicated that Mg^{2+} is six-coordinated in a Ca-Mg silicate melt, whereas it is four- and six-coordinated or a mixture of three coordination states in an Na-Mg silicate melt (Fiske and Stebbins, 1994). The relationships between the coordination states of Mg^{2+} and Fe^{2+} and the composition of melts are not exactly known at present due to the lack of sufficient structural data. It is possible, however, that Mg^{2+} in polymerized melts (with low NBO/T) is dominantly four-coordinated, but its coordination state quickly changes to six coordination with increasing NBO/T to ~1.5 and becomes nearly constant for larger NBO/T (it should be mentioned that NBO/T used here includes only Si and Al among the Ts). Because Mg^{2+} prefers six coordination relative to four coordination, magnesium in polymerized melts tends to enter olivine in which Mg^{2+} is six-coordinated. With an increase of octahedral sites in melts, Mg^{2+} enters more into melt, so that D_{Mg} decreases. In the case of Fe^{2+}, the rate of increase of six-coordinated Fe^{2+} might be smaller than that of Mg^{2+} but might decrease continuously to NBO/T > 3, resulting in the increase of K_D to NBO/T between 1.5 and 2 and the decrease with a further increase of NBO/T.

Acknowledgments—The senior author (I. K.) is grateful to the Director and other members of the Geophysical Laboratory for the invitation and use of the facilities at the laboratory and to H. Yoshida of the Geological Institute, University of Tokyo for advice on microprobe analysis. This research was partially supported by NSF grant EAR9901886 to B. O. M.

Associate editor: D. B. Dingwell

REFERENCES

Brown G. E. Jr., Farges F., and Calas G. (1995) X-ray scattering and X-ray spectroscopy studies of silicate melts. In *Structure, Dynamics and Properties of Silicate Melts* (ed. J. F. Stebbins et al.) *Rev. Mineral.* **32,** 317–410.

Carmichael I. S. E. and Ghiorso M. S. (1990) The effect of oxygen fugacity on the redox state of natural liquids and their crystallizing phases. In *Modern Methods of Igneous Petrology: Understanding Magmatic Process* (ed. J. Nicholls and J. K. Russel) *Rev. Mineral.* **24,** 191–211.

Falloon T. J., Green D. H., O'Neill H. St. C., and Hibberson W. O. (1997) Experimental tests of low degree peridotite partial melt compositions: Implications for the nature of anhydrous near-solidus peridotite melts at 1 GPa. *Earth Planet. Sci. Lett.* **152,** 149–162.

Fiske P. S. and Stebbins J. F. (1994) The structural role of Mg in silicate liquids: A high- temperature ^{25}Mg, ^{23}Na, and ^{29}Si NMR study. *Am. Mineral.* **79,** 848–861.

Ford C. E., Russell D. G., Graven J. A., and Fisk M. R. (1983) Olivine-liquid equilibria: Temperature, pressure and composition dependence of the crystal/liquid cation partition coefficients for Mg, Fe2+, Ca and Mn. *J. Petrol.* **24,** 256–265.

Gee L. L. and Sack R. O. (1988) Experimental petrology of melilite nephelinites. *J. Petrol.* **29,** 1235–1255.

Jones J. H. (1984) Temperature- and pressure-independent correlations

of olivine/liquid partition coefficients and their application to trace element partitioning. *Contrib. Mineral. Petr.* **88,** 126–132.

Kilinc A., Carmichael I. S. E., Rivers M. L., and Sack R. O. (1983) The ferric-ferrous ratio of natural silicate liquids equilibrated in air. *Contrib. Mineral. Petr.* **83,** 136–140.

Kushiro I. (2001) Partial melting experiments on peridotite and origin of mid-ocean ridge basalt. *Ann. Rev. Earth Planet. Sci.* **29,** 71–107.

Kushiro I. and Walter M. J. (1998) Mg-Fe partitioning between olivine and mafic-ultramafic melts. *Geophys. Res. Lett.* **25,** 2337–2340.

Longhi J., Walker D., and Hays J. F. (1978) The distribution of Fe and Mg between olivine and lunar basaltic liquids. *Contrib. Mineral. Petr.* **42,** 1545–1558.

Maekawa H., Maekawa T., Kawamura K., and Yokokawa T. (1991) The structural group of alkali silicate glasses determined from 29Si MAS-NMR. *J. Non-Cryst. Solids* **127,** 53–64.

Mysen B. O. (1990) Relationships between melt structure and petrologic processes. *Earth Sci. Rev.* **27,** 261–365.

Mysen B. O., Virgo D., and Seifert F. A. (1982) The structure of silicate melts: Implications for chemical and physical properties of natural magma. *Rev. Geophys.* **20,** 353–383.

Roeder P. L. and Emslie R. F. (1970) Olivine-liquid equilibrium. *Contrib. Mineral. Petr.* **29,** 275–289.

Sato M. (1972) Electrochemical measurements and control of oxygen fugacity and other gaseous fugacities with solid electrolyte system. In *Research Techniques for High Pressure and High Temperature* (ed. G. C. Ulmer), Ch. 3, Springer Verlag, New York.

Schramm C. M., DeJong B. H. W. S., and Parziale V. F. (1984) ^{29}Si magic angle spinning NMR study of local silicon environments in-amorphous and crystalline lithium silicates. *J. Am. Chem. Soc.* **106,** 4396–4402.

Sugawara T. (1998) Review on element partitioning for olivine-liquid and plagioclase-liquid (in Japanese with English abstract). *Bull. Volcanol. Soc. Japan* **43,** 181–201.

Takahashi E. (1978) Partitioning of Ni^{2+}, Co^{2+}, Fe^{2+}, Mn^{2+} and Mg^{2+} between olivine and silicate melts: Compositional dependence of partition coefficients. *Geochim. Cosmochim. Acta* **42,** 1829–1844.

Virgo D., Mysen B. O., and Kushiro I. (1980) Anionic constitution of 1-atmosphere silicate melts: Implications of the structure of igneous melts. *Science* **208,** 1371–1373.